

Estimating Battery Life in TDMA Mesh-based Wireless Sensor Networks, for Merged Data Collection Method

Gergely Sebestyén and József Kopják

Kandó Kálmán Faculty of Electrical Engineering, Óbuda University,
Bécsi út 96/b, 1034 Budapest, Hungary
sebestyen.gergely@kvk.uni-obuda.hu; kopjak.jozsef@kvk.uni-obuda.hu

Abstract: This paper provides a comprehensive description of battery life estimation and energy consumption in TDMA wireless mesh sensor networks. Specifically, we focus on the merged data collecting (MDC) method that utilizes lithium thionyl chloride batteries. We present detailed timing, energy consumption, and battery life estimation results of the MDC method in TDMA mesh sensor networks that use flooding routing. Our battery life estimation is based on actual energy consumption measurements, of the sensor nodes during various communication phases, using a realistic battery model. We also determine low-level constraints based on energy consumption measurements during different operational phases. To demonstrate the applicability of our model, we applied it to a test sensor network designed for temperature monitoring.

Keywords: wireless network energy consumption; WSN; battery life estimation; merged data collecting; MDC; IQRf; FRC; TDMA; flooding routing

1 Introduction

Wireless sensor networks are increasingly being used in food manufacturing for process monitoring and quality assurance. In compliance with HACCP requirements that mandate daily temperature recording in manufacturing facilities and storage spaces. In such facilities, sensor networks are designed to automate temperature recording without disrupting the manufacturing process or generating dust. As a result, wireless sensors with battery power supplies are often the best option. However, accurate battery life estimation is crucial for planning maintenance periods in field applications. Energy consumption reduction is one of the biggest challenges in battery-powered wireless sensor networks. This paper proposes a battery life estimation method for TDMA mesh-based wireless sensor networks (WSNs) utilizing merged data collection technique.

TDMA-based wireless mesh sensor networks are widely utilized in industrial fields due to their deterministic media access. Popular network technologies such as WirelessHART or ISA-100 utilize graph routing for efficient point-to-point routing [17-20]. Various studies have discussed energy consumption estimation for these networks [34-37].

The IQRF network technology relies on flooding routing to send broadcast messages across other networks. Although flooding routing is not the most efficient method for point-to-point messaging, it is a reliable and efficient technique for sensor data collection in wireless sensor networks (WSNs), especially when using the merged data collection method. In previous studies, we have highlighted the benefits of merged data collection in TDMA WSNs [1] and introduced a deep sleep algorithm that reduces the energy consumption of sensor nodes [2].

The optimal network topology for a specific use case depends on the RF (Radio Frequency) range of the wireless technology being used. The star topology is the simplest wireless topology and is suitable for point-multipoint networks, as long as the RF range of the gateway can cover the entire facility [6] [7] [22]. However, in cases where sensors are located in a cold storage built from metal materials, the RF range of low-power wireless devices may not cover the entire facility. In such cases, mesh or tree network topologies enable nodes to route communication messages throughout the network, thereby extending the RF range of the entire network. In a mesh or tree network topology, nodes retransmit received packets through the routing procedure, and the number of message retransmissions is measured in hops, where each hop represents one retransmission [15]. Multi-hop wireless mesh communication technology can efficiently cover the entire manufacturing area.

Figure 1 illustrates a sensor network application installed in a manufacturing facility. The objective of this sensor network is to automatically collect data from sensor nodes in compliance with HACCP requirements, which mandate the daily recording of temperature. However, some companies may need oversampling for quality assurance purposes every hour or even every 15 minutes [5]. In IQRF networks, the discovery process assigns a Virtual Routing Number (VRN) to nodes within the network. A breadth-first search algorithm is used during the discovery process to lease VRN addresses. The VRN address indicates the routing distance from the network coordinator and defines the dedicated time slot for nodes during the routing procedure [15] [22]. Figure 2 displays the network graph for the test network, along with the logical addresses and VRNs.

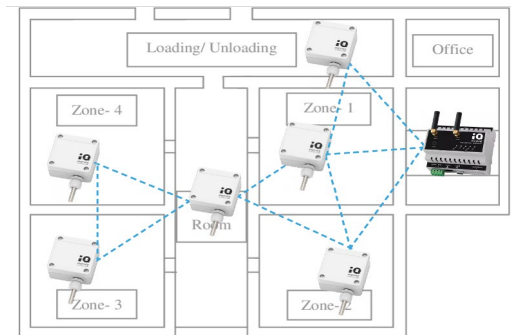


Figure 1

Installed test sensor network

Temperature values can be recorded in a wireless sensor network by collecting data from the sensor nodes. The data collection can be initiated either by the sensor nodes themselves or by the network coordinator. If the sensors initiate data transmission, it is asynchronous with the rest of the network. This can lead to collisions in TDMA networks due to possible time slot overlapping. However, collisions can be avoided through synchronization.

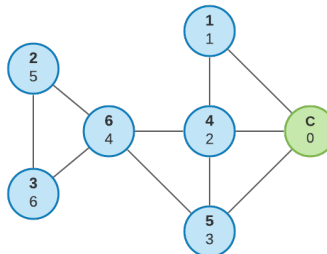


Figure 2

Wireless mesh sensor network graph with logical addresses (top) and VRNs bottom)

There are several ways to implement synchronization in a sensor network. One option is to use super frames, similar to WirelessHART networks [17]. Another approach is to use a request-response pattern where the data collection is centralized and the wireless network coordinator always initiates communication. With this approach, the sensor nodes don't require additional synchronization for network initialization. Centralized data collection simplifies the process and eliminates the possibility of synchronization issues.

2 Merged Data Collection Methods for Wireless Sensor Networks

Flooding routing can be a slow but robust and reliable routing mechanism, especially in dense routing networks. In a previous paper [1], we compared different data collection methods in IQRF-like networks. Our test sensor network demonstrated the usefulness of simultaneous data collection, and we compared centralized data collection methods like polling, synchronized broadcast response, and merged data collection. We evaluated these methods based on the duration and number of transmissions per node.

The merged data collection method leverages flooding routing in TDMA mesh networks. The concept is to send measured sensor values in one response packet as a broadcast request to the entire network. This method works best when a small amount of data is collected from each node. The message payload size depends on the number of nodes collecting sensor data. For temperature sensor data, this method only collects one byte from each node. In IQRF, the payload size is 64 bytes, which can collect merged data from a maximum of 64 nodes [10].

The merged data collection method begins with a request broadcast packet. When the last node receives this packet, it transmits its response in its time slot. Other nodes continue to transmit sensor data in their designated time slots, similar to flooding routing. Each node merges the received packet payloads and inserts their own measured value into the appropriate byte in the payload based on the address. When the coordinator receives the final packet and merges it, the measured sensor data is available at the designated byte in the packet payload.

IQRF's implementation of the Fast Response Command (FRC) extends the data merging algorithm by including an additional non-routing packet transmission. Before the response is routed through the network, each node sends its own data as a beacon message. This transmission allows all neighboring nodes to receive the sensor data of the node. The non-routing packet is intended to support non-routing devices that lack a VRN number and is sent in a time slot based on the logical addresses of the nodes. In a fully discovered network, this results in duplicated transmission of responses, which enhances the reliability of data collection [15] [22-24]. The duration of merged data collection varies depending on the network size:

$$t_{MDC} = N(t_{req} + t_{MDCresp}) + t_{proc} \quad (1)$$

where $t_{MDCresp}$ is the time slot of the response packets. As per the IQRF specification [15], the larger packet size causes a longer time slot due to the increased propagation time. Therefore, the merged data collection method has a time complexity of $O(N)$, where N represents the number of nodes in the network.

Compared to merged data collection, the Fast Response Command (FRC) with additional data transmission has a longer duration. The duration of FRC data collection in a fully discovered network is [15] [16]:

$$t_{FRC} = N \cdot t_{req} + t_{FRCresp}(N + 2) + t_{proc} + t_{Cproc} \quad (2)$$

As depicted in Figure 3, the merged data collection method is significantly faster than polling or synchronized response in larger networks.

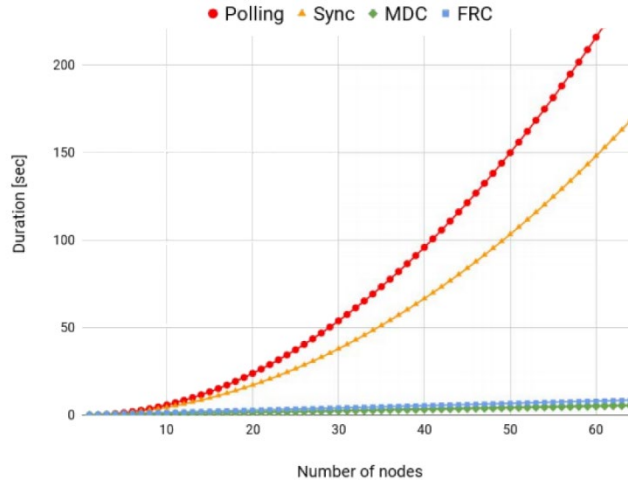


Figure 3

Duration of data collecting methods based on the TR-76D timings [16]

3 Sensor Node Energy Consumption in Wireless Sensor Networks Using Merged Data Collection Methods

In order to estimate the battery life of sensor nodes, we first needed to define their energy consumption when using Merged Data Collection (MDC) methods. For this purpose, we used the Fast Response Command (FRC) method, which we found to be more reliable in field applications, as we have previously described in [1]. Furthermore, the energy consumption of MDC can be reduced by removing the non-routing beacon sending phase. To simplify the energy consumption estimation, we replaced low-level constraints, such as hardware and driver limitations, with actual measured energy costs. In Wireless Sensor Networks (WSNs), high-level constraints, such as network communication, have a significant impact on energy consumption. The communication cycle of sensor

nodes can be divided into well-defined phases, as shown in the current diagram of two sensor nodes in Figure 2. The phases are:

- Deep sleep
- Idle
- Request Broadcast Message Routing
- Processing: reading sensor values
- Sending non-routing beacon packets
- Response message routing

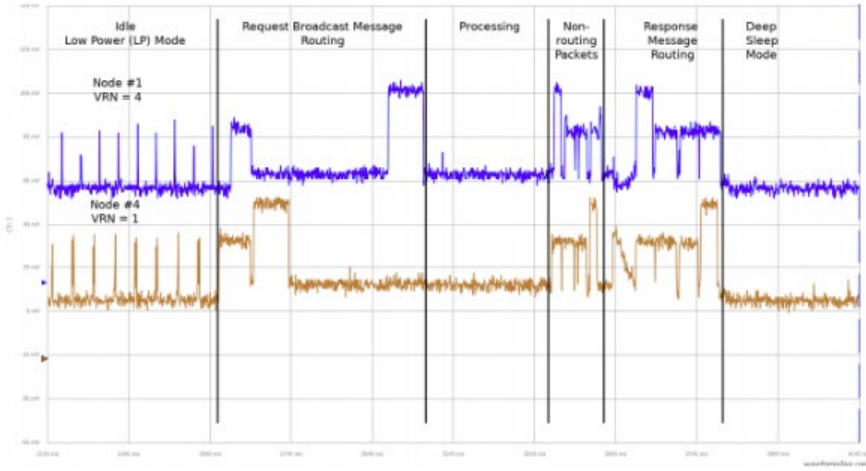


Figure 4

Measured current of TR-76D modules divided into phases [16] of nodes 1 and 4 during FRC data collecting method

Nodes in the idle state are capable of receiving incoming messages. Upon receiving a request message, each node repeats it in its own time slot as defined by flooding routing. Once the packet transmission is complete, the node disables its transceiver module to avoid receiving anything until the end of the routing. This ensures that each node in the network receives the message. In the next processing phase, the nodes can process the incoming request, acquire sensor data, and must complete this task within a predefined time.

The total energy consumption of a sensor using synchronized deep sleep:

$$E_{total} = n_r E_{FRC} + E_{dsleep} \quad (3)$$

The total energy consumption of the FRC merged data collecting method can be calculated as the sum of the energy consumption in each phase:

$$E_{FRC} = E_{idle} + E_{request} + E_{proc} + E_{beacon} + E_{response} \quad (4)$$

Table 1
Variables used in the energy consumption model described in this paper

Variable	Description
E_{total}	Energy consumption of the node
E_{FRC}	Energy consumption of FRC data collecting cycle
E_{idle}	Energy consumption in idle mode
$E_{request}$	Energy consumption of the request broadcast routing
E_{proc}	Energy consumption of message processing and sensor acquisition
E_{beacon}	Energy consumption of the beacon sending
$E_{response}$	Energy consumption of the response routing
E_{dsleep}	Energy consumption of deep sleep mode
U	System voltage
I_{Rx}	Current of RF receive mode
I_{Tx}	Current of RF transmission mode (at max output power)
I_{LP}	Current of idle LP mode
N	Number of network nodes without the coordinator
n_r	Number of requests per data collecting cycle
t_{req}	Timeslot for request message
t_{resp}	Timeslot of response message
t_p	Duration of synchronization preamble
t_{proc}	Message processing time
t_{dsleep}	Duration of deep sleep mode
t_{qsleep}	Sleep quantum (2.097s at IQRF deep sleep)
t_{period}	Periodic request interval
t_{FRC}	Total duration of FRC data collecting
t_{idle}	Duration of idle mode before FRC request
t_{bc}	Duration of beacon non-routing
t_{bcw}	Pause after beacon sending

We make the assumption that the power supply circuit is shared among the sensor components, and the system voltage level is dependent on both the discharge characteristics of the lithium thionyl chloride batteries and the voltage regulator applied in the sensor node, as described in references [15] [26].

Deep Sleep Mode

In a previous paper [2], we described the synchronized deep sleep mode as a technique for extending battery life in sensor networks that use centralized data collection. This mode reduces energy consumption by disabling the transceiver module and putting the sensor nodes into deep sleep mode until the next data collection period. As depicted in Figure 2, the deep sleep mode is activated simultaneously in all nodes after the FRC data collection is completed. The duration of the deep sleep period is determined by the system's requirements and is typically optimized for energy savings. The deep sleep time is:

$$t_{dsleep} = t_{period} - t_{FRC} \quad (5)$$

To ensure stable communication, it is crucial for sensor nodes to switch from active to idle mode before receiving requests in the next data collection cycle. If a sensor misses a request, it remains in idle mode until the next one, leading to increased energy consumption. Moreover, it is essential to ensure that the sleep time is shorter than the period time. Figure 5 illustrates the proper and improper operations of the synchronized deep sleep algorithm. In case a node misses a request, it cannot route the packet, leading to network communication failures. Therefore, it is vital to minimize the occurrence of missed requests and optimize the sleep time to ensure efficient and reliable communication.

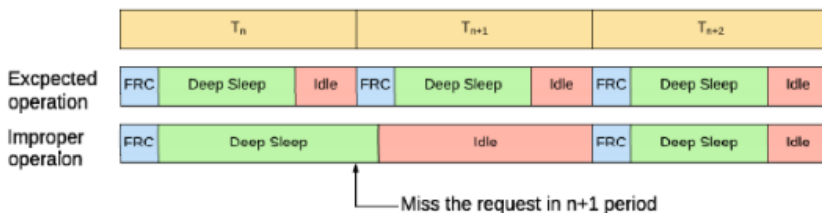


Figure 5

Expected and improper operation of deep sleep mode

To ensure that all sensor nodes are in the idle state before the next request is transmitted from the network coordinator, it is necessary to calculate a deep sleep time that is shorter than the period time. This is because all nodes must be in the idle state before the request is sent.

The deep sleep time calculation is based on the worst-case wake-up times of the sensor nodes. To determine the deep sleep time, we measured the sleep time and identified the maximum differences between the wake-up times of the nodes. We then used these maximum values to fit a linear regression, as shown in Figure 5. Using this regression, we can calculate the deep sleep time of the sensor nodes in seconds, as follows:

$$t_{dsleep} = (t_{period} - t_{FRC}) - 0.00219 \cdot (t_{period} - t_{FRC}) + 2.70629 \quad (6)$$

where t_{period} is the time until the next data collecting period and t_{FRC} is the duration of the data collecting communication. To ensure proper synchronization using the deep sleep method, it is important to calculate the inaccuracy of the internal clock of the radio modules.

Idle Mode

The IQRF technology incorporates a method known as Low Power Receive (LP-RX) mode, which aims to minimize power consumption by periodically disabling the receive mode and shutting down the transceiver module. Specifically, the LP-RX mode defines a period of 47 milliseconds for IQRF devices, during which the radio module attempts to detect incoming RF packets.

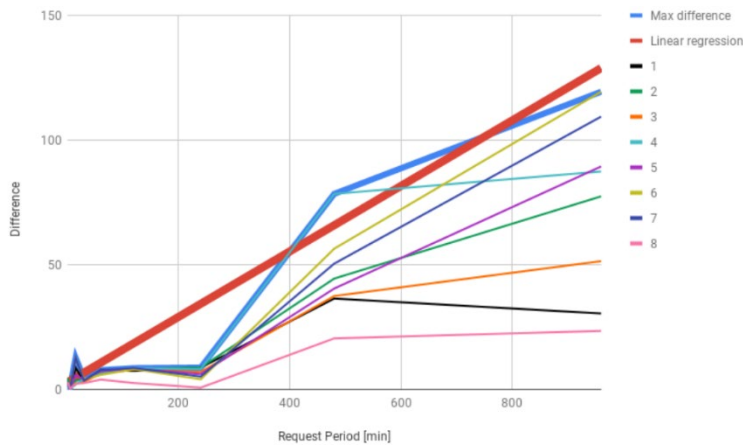


Figure 6

Expected and improper operation of deep sleep mode of IQRF modules

To signal the start of a packet, the sender node transmits a 50-millisecond long preamble that can be detected by the receiver nodes. Once the preamble is detected, the receiver stays in receiver mode to receive the rest of the network packet. Compared to the standard receiving mode, the LP idle mode power consumption in a noise-free RF environment is only about two percent, which can lead to significant energy savings for battery-powered devices.

However, even in LP-RX mode, the RF circuitry may still consume some power due to synchronization needs or other factors. Therefore, the use of synchronized deep sleep mode can further reduce the energy consumption of the sensor nodes, especially in cases where the request periods are longer. In contrast, the normal RF receive mode keeps the RF circuitry on all the time, which can lead to higher energy consumption and shorter battery life. Overall, the LP-RX mode is a useful feature of IQRF technology that enables efficient and reliable communication while minimizing power usage [15] [16].

In the test nodes, the IQRF RF modules utilize a watchdog timer in conjunction with a low power oscillator to control the timing of the deep sleep mode. This timer covers a wide range of sleep intervals, allowing IQRF to define the deep sleep quantum as $t_{qsleep}=2.097$ s, which is based on the properties of the microcontroller being used [13]. During this deep sleep mode, the device is in an idle state and is able to conserve power by shutting down non-essential functions. The duration of the idle state can vary based on the specific application and usage scenario:

$$t_{idle} = t_{period} - t_{FRC} - \lfloor t_{dsleep} / t_{qsleep} \rfloor \cdot t_{qsleep} \quad (7)$$

where t_{dsleep} is the deep sleep time of the sensor nodes taking into account oscillator inaccuracies. The energy consumption of the idle state can be

determined using the average current for low power (LP) mode, represented by ILP, as follows:

$$E_{idle} = UI_{LP}t_{idle} \quad (8)$$

where I_{LP} is the average current for LP mode by IQRF.

Request Broadcast Message Routing

The FRC (Fast Response Communication) method begins with a request broadcast message, which is sent out to all nodes in the network. Each node then repeats the packet in their own designated time slot and subsequently disables their transceiver module, as they do not need to receive any more packets until the end of the routing process. By repeating the packet in this way, each node in the network is able to receive the message, ensuring that it is delivered to all intended recipients. This approach can be an efficient way to quickly disseminate information throughout a network, as it allows for the simultaneous transmission of data to multiple nodes without requiring individual requests or acknowledgments. Overall, the FRC method is a useful tool for enabling fast and reliable communication within a network. The energy requirement of the request phase is:

$$E_{request} = U(I_{Rx}(t_p + t_{req}) + (N - 2) \cdot I_{idle}(t_p + t_{req}) + I_{Tx}(t_p + t_{req})) \quad (9)$$

Processing

Once the request message is received by all network nodes, they begin processing the acquired sensor data and preparing it for collection. In the test network, the sensor nodes utilize a low-power digital temperature sensor which consumes less energy than the idle mode energy consumption of the RF circuits. This helps conserve energy while ensuring efficient data collection. The energy requirement of the request phase is:

$$E_{proc} = U(I_{idle}t_{proc}) + E_{sensor} \quad (10)$$

Non-Routing Beacon Packets

During the upcoming phase of the FRC, each node will transmit its sensor data to neighboring nodes during designated time slots. To receive data from all neighbors, each node must remain in receive mode until all other nodes have transmitted their packets. Once the packets are received, the nodes will merge the payload data based on their respective network addresses and include their own measured values. The energy consumption of the beacon phase is:

$$E_{beacon} = U(I_{Rx}(N - 1)t_{bc} + I_{Tx}t_{bc} + I_{idle}t_{bcw}) \quad (11)$$

To ensure proper communication, each node must remain in receive mode for N-1 time slots to receive data from other nodes, and then one additional time slot to

transmit data to its neighbors. Following the beacon phase, the nodes will wait a short t_{bcw} time slot before proceeding with data transmission.

Response Message Routing

The response message routing phase begins with the node having the highest VRN number transmitting the merged payload. The network nodes will then route the response message payload towards the data concentrator by repeating it in decreasing order of VRN numbers. Each node will merge the payloads before routing the packet. As a result, when the data concentrator receives the last packet and merges it, all measured data from all sensor nodes can be found at the appropriate location within the response message payload. The energy consumption associated with the beacon response message routing process is:

$$E_{response} = U(I_{Rx}t_{resp}(N-1) + I_{Tx}t_{resp}) \quad (12)$$

To receive incoming messages, nodes must remain in receive mode for $N-1$ time slots, as is the case during the beacon phase. After receiving messages, nodes need to transmit their own message in a single time slot.

4 Estimated Battery Life of the Sensor Nodes

The lifetime of the network is determined by the first node that becomes unable to communicate [28] [32] [34]. Typically, the network's lifetime is defined as the moment when the first sensor becomes inoperable due to low battery. This is a commonly accepted definition of network lifetime.

To estimate the battery lifetime of a sensor node based on its energy consumption, the following steps can be taken:

- Calculate the total energy consumption (E_{total}) of the node by using a suitable model and determining the average current to define the appropriate discharge characteristic of the battery.
- Determine the maximum number of data collecting cycles that can be served from the battery capacity, using the proper battery discharge characteristic.
- Calculate the estimated battery lifetime from the maximum number of data collecting cycles and request period.

The total energy consumption of the node depends on several factors, including the number of nodes in the network, data collecting period, and the number of data collecting requests in each period.

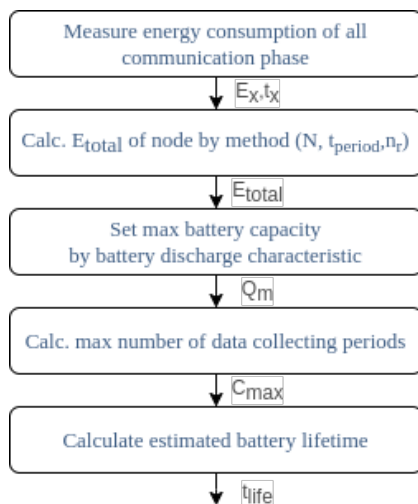


Figure 7

The total energy consumption (E_{total}) of a node for one data request per period

Figure 8, illustrates the total energy consumption of a sensor node in the case of one data request per period, based on the parameters of the TR-76D module [16].

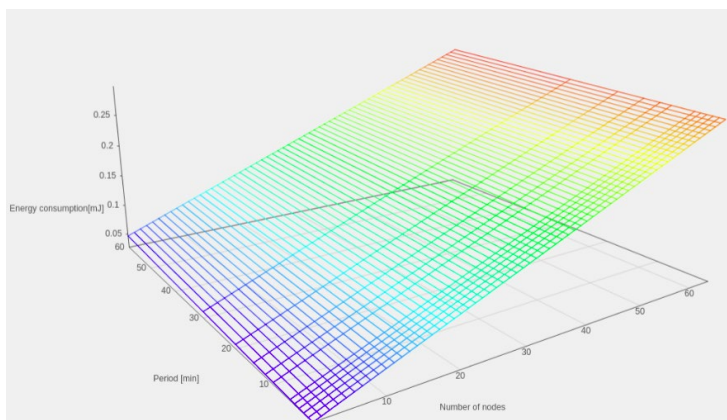


Figure 8

The total energy consumption (E_{total}) of a node for one data request per period

To estimate the battery lifetime, we need to determine the maximum number of data collecting cycles that can be supported by the battery's capacity. While lithium thionyl chloride (Li/SOCl_2) batteries have high capacity, high energy density, and low self-discharge rates, their output current capability is limited. Additionally, the battery's capacity varies significantly depending on the discharge rate. Despite these limitations, Li/SOCl_2 batteries are still an ideal choice for long-term running applications [30].

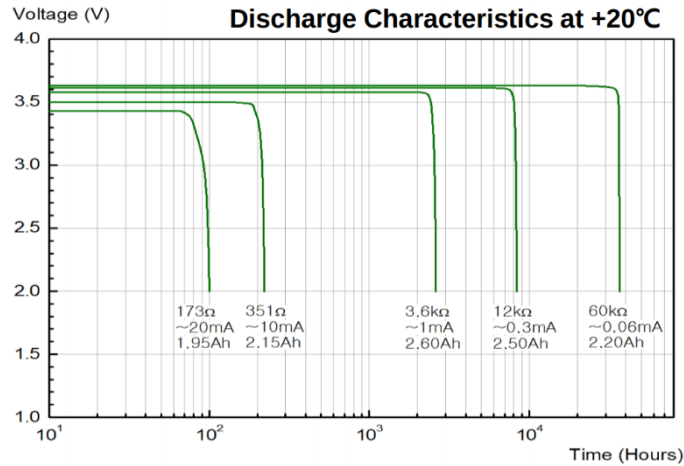


Figure 9

Discharge characteristic of Li/SOCl₂ battery [26]

The capacity of a battery depends on the average energy consumption and can be determined by analyzing the battery's discharge characteristics while considering its maximum pulse current capability. Figure 9 illustrates the discharge characteristics of a Li/SOCl₂ battery at different loads. Additionally, the battery's self-discharge characteristics are affected by the load and can impact its expected lifetime. After 10 years of discharging to 90% of its nominal capacity, a Li/SOCl₂ battery typically retains a capacity that reflects its discharge characteristics. Notably, the self-discharge rate of a Li/SOCl₂ battery is extremely low, less than 1% per year at 20°C, which enables long storage periods and a service life of 10 to 20 years[29].

One of the primary challenges with this type of battery is that when it comes into contact with SOCl₂, the lithium rapidly reacts to form a passivation layer that can slow down further corrosion reactions. This affects the battery's lifetime, which depends on various factors, including the storage time and environmental conditions between manufacturing and the battery's use in sensors. Due to the complexity of the factors that influence the Li/SOCl₂ battery's self-discharge rate, it is challenging to establish an accurate mathematical life prediction model for this type of battery[30]. Despite these challenges, the maximum number of data collection cycles that can be supported by the battery's capacity during its' lifetime is:

$$c_{\max} = \left\lfloor \frac{Q_m U}{E_{\text{total}}} \right\rfloor \quad (13)$$

where Q_m represents the battery's capacity, which is determined based on the discharge characteristics at the end of the battery's life.

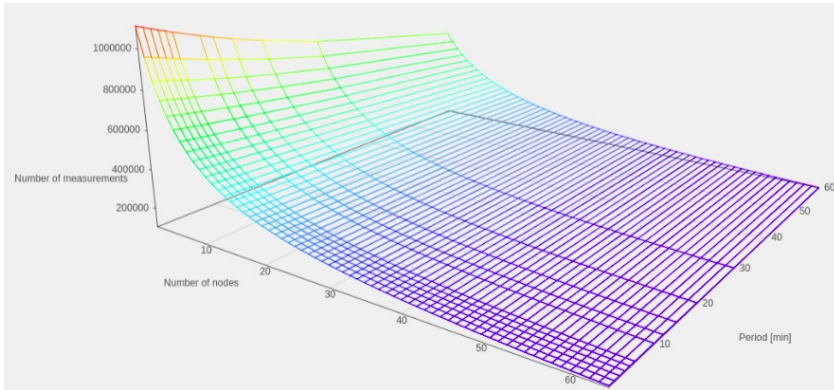


Figure 10

Maximum number of data collecting cycles that can be served from the battery capacity

Figure 10 illustrates the nominal battery capacity, which can be used to determine the maximum number of data collection cycles that the battery can support. By calculating the maximum number of data collection cycles, we can estimate the battery's lifetime:

$$t_{life} = C_{max} t_{period} \quad (14)$$

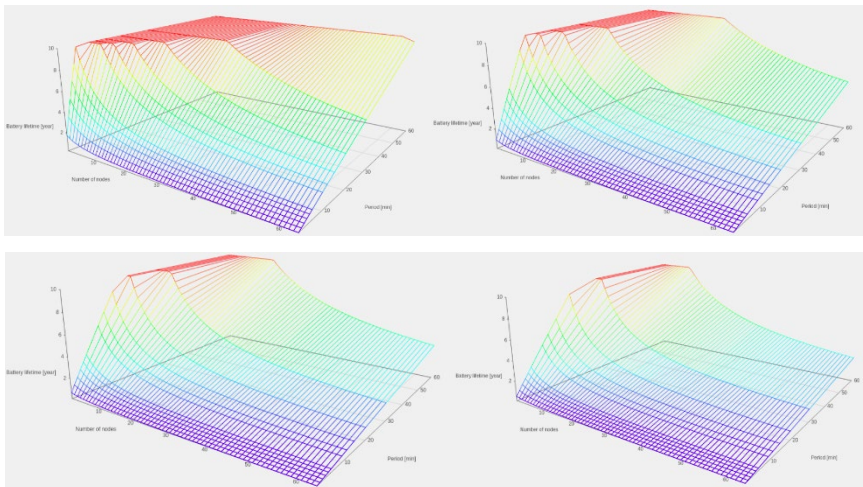


Figure 11

Estimated battery lifetime at up to 4 request per cycle

Based on the parameters of the TR-76D module, Figure 11 depicts the estimated battery lifetime for up to four requests per data collection cycle and a maximum lifetime of 10 years. The diagrams demonstrate that increasing the number of nodes in the network or collecting data more frequently can significantly reduce

the battery's lifetime. However, increasing the number of nodes in the network can be offset by decreasing the data collection interval.

To validate the model, we conducted short-term testing using a test sensor network. Additionally, we initiated a long-term test using six sensor nodes, which will span over five years. However, the long-term test may yield different results due to the Li/SOCl₂ battery's capacity characteristics. In the test sensor network used for model validation during short-term testing, we employed:

- 3 sensor nodes (IQ Home SI-T-02) [27]
- XL-060F batteries from the same batch [26]
- 1 minute data collecting period with 2 requests per period (temperature + status)
- Estimated battery life by the model: 207 days

As previously defined, the lifetime of the sensor network is determined by the first inoperable sensor node. However, in our test networks, we wanted to observe the battery life of all sensor nodes, not just the first one to fail. To achieve this, we set up the sensor network with each sensor node having a direct link to the coordinator. This design ensures that network communication is not interrupted in the event of any node ceasing to function. By observing the battery life of all sensor nodes in the network, we can gain a more comprehensive understanding of the overall performance and durability of the sensor network.



Figure 12

Temperature values until the end of battery life in short-term test network

Figure 12 shows the temperature values collected during the short-term test network. The test lasted 245 days until the last sensor node's battery became low. Table 2 presents the results of the battery life test. The primary objective was to validate the estimated battery life of each sensor node, and each node worked until the estimated time. However, the significant difference between the results can be attributed to the Li/SOCl₂ batteries used, even though they were from the same

batch and order, and stored under similar conditions. This variance emphasizes the importance of testing and validating battery life to ensure accurate and reliable sensor network performance.

Table 2
Results of the short-term battery life estimation test

Node	Estimated battery life (days)	Battery life (days)	Error
1(green)	207	216	+4.35%
2(red)	207	208	+0.48%
3(grey)	207	245	+18.36%

5 Energy Consumption Distribution in the Network

The energy consumption distribution of a wireless network depends on the specific architecture and data collection methods employed [29-32]. Assuming a homogeneous network with identical sensor and battery types, variations in energy consumption can be attributed solely to the communication costs of the data collection method. Therefore, it is crucial to understand the energy consumption distribution as it directly impacts the network's lifetime. Any node with higher communication energy costs than the others may become inoperable sooner, potentially causing communication issues. This is because the network's lifetime is determined by the first node that becomes inoperable.

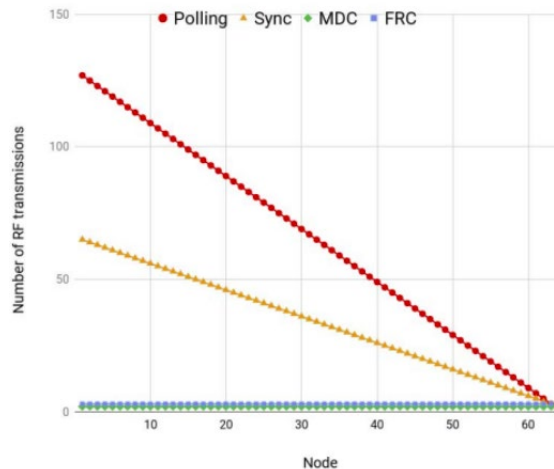


Figure 13

The distribution of number of transmissions at different data collecting methods in a 64-node network

In TDMA wireless mesh sensor networks that utilize flooding routing, the merged data collection (MDC) method results in uniform communication energy costs across all nodes, regardless of their location in the network. This is because routing nodes must transmit messages to the same number of nodes, regardless of their location, when using MDC methods. Figure 13 illustrates the number of transmissions required by different data collection methods in a network with 64 nodes. The energy consumption model of sensor nodes using MDC methods depends only on the total number of nodes in the network, and not on their location.

Conclusions

This paper presents an energy consumption estimation method, for sensor nodes in TDMA wireless mesh sensor networks, that utilize FRC merged data collecting methods and lithium thionyl chloride batteries. We describe a battery life estimation method, which we validated through short-term testing using a test sensor network. The battery life of a sensor node in a homogeneous network depends on three factors: the number of nodes in the network, the data collection period, and the number of data collection requests in each period. By decreasing the data collection interval, the battery life estimation method can compensate for the increasing number of nodes in the network. We also demonstrate that the communication energy cost of nodes using merged data collecting methods in TDMA wireless mesh sensor networks, based on flooding routing, is uniform across all nodes, regardless of their location within the network.

References

- [1] J. Kopják and G. Sebestyén, "Comparison of data collecting methods in wireless mesh sensor networks," 2018 IEEE 16th World Symposium on Applied Machine Intelligence and Informatics (SAMi), Kosice, 2018, pp. 155-160
- [2] J. Kopjak and G. Sebestyén, "Deep sleep algorithms in battery powered TDMA wireless mesh sensor network," 2018 IEEE 18th International Symposium on Computational Intelligence and Informatics (CINTI) 2018, pp. 000115-000118
- [3] J. Kopják and G. Sebestyén, "Energy Consumption Model of Sensor Nodes using Merged Data Collecting Methods," 2022 IEEE 20th Jubilee World Symposium on Applied Machine Intelligence and Informatics (SAMi), Poprad, Slovakia, 2022
- [4] G. Sebestyén and J. Kopják, "Battery Life Prediction Model of Sensor Nodes using Merged Data Collecting methods," 2022 IEEE 20th Jubilee World Symposium on Applied Machine Intelligence and Informatics (SAMi) Poprad, Slovakia, 2022
- [5] K. Likar, M. Jevšnik, "Cold chain maintaining in food trade," In Food Control, Volume 17, Issue 2, 2006, pp. 108-113

-
- [6] Sharma, D. & Verma, Sandeep & Sharma, K. (2013) Network topologies in wireless sensor networks: A review. *Int. J. Electron. Commun. Technol.* 4. 93-97
- [7] Zhang, D., Zhu, Y., Zhao, C., & Dai, W. (2012) A new constructing approach for a weighted topology of wireless sensor networks based on local-world theory for the Internet of Things (IOT). *Computers & Mathematics with Applications*, 64(5), 1044-1055
- [8] Bouguera, T.; Diouris, J.-F.; Chaillout, J.-J.; Jaouadi, R.; Andrieux, G. Energy Consumption Model for Sensor Nodes Based on LoRa and LoRaWAN. *Sensors* 2018, 18, 2104
- [9] D. Tudose, L. Gheorghe, and N. Tăpuș, "Radio transceiver consumption modeling for multi-hop wireless sensor networks," *UPB Sci. Bull. Ser. C Electr. Eng.*, Vol. 75, No. 1, pp. 17-26, 2013
- [10] J. Song and Y. K. Tan, "Energy consumption analysis of ZigBee-based energy harvesting wireless sensor networks," 2012 IEEE International Conference on Communication Systems (ICCS), 2012, pp. 468-472
- [11] V. Agarwal, R. A. DeCarlo, and L. H. Tsoukalas, "Modeling Energy Consumption and Lifetime of a Wireless Sensor Node Operating on a Contention-Based MAC Protocol," in *IEEE Sensors Journal*, Vol. 17, No. 16, pp. 5153-5168, 15 Aug. 15, 2017
- [12] Yunxia Chen and Qing Zhao, "On the lifetime of wireless sensor networks," in *IEEE Communications Letters*, Vol. 9, No. 11, pp. 976-978, Nov. 2005
- [13] Z. Cheng, M. Perillo and W. B. Heinzelman, "General Network Lifetime and Cost Models for Evaluating Sensor Network Deployment Strategies," in *IEEE Transactions on Mobile Computing*, Vol. 7, No. 4, pp. 484-497, April 2008
- [14] Accurate Online Estimation of Battery Lifetime for Wireless Sensors Network (2013) Proceedings of the 2nd International Conference on Sensor Networks
- [15] IQRF Tech s.r.o., "IQRF OS User's Guide Version 4.03D for (DC)TR-7xD", 2018, https://www.iqrfalliance.org/data_files/news/user-guide-iqrf-os-403d-tr-7xd-181025.pdf
- [16] IQRF Tech s.r.o., "TR-76D RF Transceiver Module Series Data Sheet", 2021, https://static.iqrf.org/Datasheet_TR-76D_210712.pdf
- [17] F. Li, Z. Zhang, Z. Jia, and L. Ju, "Superframe Scheduling for Data Aggregation in WirelessHART Networks," 2015 IEEE 17th International Conference on High Performance Computing and Communications, 2015 IEEE 7th International Symposium on Cyberspace Safety and Security, and

- 2015 IEEE 12th International Conference on Embedded Software and Systems, New York, NY, 2015, pp. 1540-1545
- [18] "SmartMesh WirelessHART - Linear Technology," Linear.com, 2017 [Online] Available: <https://www.analog.com/en/applications/technology/smartmesh-pavilion-home/smartmesh-wirelesshart.html> [Accessed:2020-Dec-6]
- [19] ANSI/ISA-100.11a-2011 Wireless systems for industrial automation: Process control and related applications, ISA, January 2022
- [20] Nixon, M. and Rock, T.R., 2012. A Comparison of WirelessHART and ISA100. 11a. Whitepaper, Emerson Process Management, pp. 1-36
- [21] ZigBee Alliance, "ZigBee: ZIGBEE SPECIFICATION," [Online]
- [22] P. Seflova, V. Sulc, J. Pos and R. Spinar, "IQRf wireless technology utilizing IQMESH protocol," 2012 35th International Conference on Telecommunications and Signal Processing (TSP) Prague, 2012, pp. 101-104
- [23] R. Kuchta, R. Vrba and V. Sulc, "Smart Platform for Wireless Communication - Case Study," Seventh International Conference on Networking (icn 2008) 2008, pp. 117-120
- [24] V. Sulc, R. Kuchta and R. Vrba, "IQMESH Implementation in IQRf Wireless Communication Platform," 2009 Second International Conference on Advances in Mesh Networks, 2009, pp. 62-65
- [25] Cheng, S., Li, B., Yuan, Z., Zhang, F., & Liu, J. (2016) Development of a lifetime prediction model for lithium thionyl chloride batteries based on an accelerated degradation test. *Microelectronics Reliability*, 65, 274-279
- [26] XENO-ENERGY Co. Ltd., XL-060F Li/SOCl₂ battery datasheet, http://www.xenoenergy.com/eng/file/Xeno%20Catalog%20XL-060F_E.pdf
- [27] IQ Home, Industrial Temperature Sensor [SI-T-02] <https://www.iqhome.org/SI-T-02>
- [28] Jae-Hwan Chang and L. Tassiulas, "Energy conserving routing in wireless ad-hoc networks," Proceedings IEEE INFOCOM 2000. Conference on Computer Communications. Nineteenth Annual Joint Conference of the IEEE Computer and Communications Societies (Cat. No.00CH37064) 2000, pp. 22-31, Vol. 1
- [29] GlobTek, Inc. globtek.com, 2021 [Online] Available: <https://en.globtek.com/lithium-thionyl-chloride-li-socl2-batteries>. [Accessed:2021-Feb-8]
- [30] Texas Instruments, Tech Note: How to Extend Operating Time of a LiSOCl₂ Powered System, <https://www.ti.com/lit/an/slvaev9/slvaev9.pdf>

-
- [31] Abbas, M., & Otayf, N. (2021) A novel methodology for optimum energy consumption in wireless sensor networks. *Frontiers in Engineering and Built Environment*, 1(1), 25-31
- [32] M. Srbinovska, V. Dimcev and C. Gavrovski, "Energy consumption estimation of wireless sensor networks in greenhouse crop production," *IEEE EUROCON 2017, 17th International Conference on Smart Technologies*, 2017, pp. 870-875
- [33] Zhou, C., Wang, M., Qu, W., & Lu, Z. (2018) A Wireless Sensor Network Model considering Energy Consumption Balance. *Mathematical Problems in Engineering*, 2018, 1-8
- [34] Elshrkaway, M., Elsherif, S. M., & Elsayed Wahed, M. (2018) An Enhancement Approach for Reducing the Energy Consumption in Wireless Sensor Networks. *Journal of King Saud University - Computer and Information Sciences*, 30(2), 259-267
- [35] Muller, I., Winter, J. M., Brusamarello, V., Pereira, C. E., & Netto, J. C. (2014) Algorithm for estimation of energy consumption of industrial wireless sensor networks nodes. *2014 IEEE International Instrumentation and Measurement Technology Conference (I2MTC) Proceedings*
- [36] Nikolaos A. Pantazis; Dimitrios J. Vergados; Dimitrios D. Vergados; Christos Douligeris (2009) Energy efficiency in wireless sensor networks using sleep mode TDMA scheduling, 7(2), 322-343
- [37] Muller, Ivan; Winter, Jean; Pereira, Carlos; Brusamarello, Valner; Netto, Joao C. (2016) 2016 IEEE 14th International Conference on Industrial Informatics (INDIN) - Energy consumption estimation for TDMA-based industrial wireless sensor networks
- [38] Combining fuzzy signature and rough sets approach for predicting the minimum passing level of competency achievement (*Int. J. Artif. Intell.* 18(1): 237-249 (2020))
- [39] Evolving fuzzy models for prosthetic hand myoelectric-based control (*IEEE Trans. Instrum. Meas.* 69(7): 46250-4636 (2020)) A unified form of fuzzy C-means and K-means algorithms and its partitional implementation (*Knowl.-Based Syst.* 214: 106731 (2021))
- [40] Tensor product-based model transformation approach to tower crane systems modeling, *Asian Journal of Control*, Vol. 23, No. 3, pp. 1313-1323, 2021
- [41] Modelling, forecasting and testing decisions for seasonal time series in tourism, *Acta Polytechnica Hungarica*, Vol. 17, No. 10, pp. 149-171, 2020
- [42] Analysis of human activities and identification of uncertain situations in context-aware systems, *International Journal of Artificial Intelligence*, Vol. 18, No. 2, pp. 135-154, 2020